Received February 12, 2020, accepted February 28, 2020, date of publication March 5, 2020, date of current version March 17, 2020.

Digital Object Identifier 10.1109/ACCESS.2020.2978497

Group-Wise Listen-Before-Talk Protocol for Dynamic Spectrum Sharing: A New Framework for Full Frequency Reuse

CHAN S. YANG AND CHUNG G. KANG, (Senior Member, IEEE)
Department of Electrical Engineering, Korea University, Seoul 02841, South Korea

Corresponding author: Chung G. Kang (ccgkang@korea.ac.kr)

This work was supported by the Samsung Research in Samsung Electronics.

ABSTRACT In existing dynamic spectrum sharing (DSS) systems, each node arbitrates channel access independently based on carrier-sensing mechanisms such as the listen-before-talk (LBT) protocol. Owing to the uncoordinated channel access between all nodes, the channel is occupied in a random pattern. This makes it difficult to reduce the mismatch in channel quality indicator (CQI) while increasing the spatial reuse gain between the different nodes; therefore, the areal capacity gain obtained by adding nodes is much lower in existing DSS systems than in the cellular system. In this paper, we propose a different means of improving the areal capacity for downlink DSS systems. It is a group-wise DSS approach that ensures full frequency reuse in each group of base stations (BSs) by performing LBT only between the representative BSs, each of them selected by each group. Once a channel is secured by each group, all its member BSs share a channel simultaneously. This approach makes closed-loop feedback-based link adaptation practical while boosting spatial reuse gain even in the DSS environment. To implement the group-wise DSS, we propose a single unified framework that employs elementary algorithms for BS grouping and carrier-sensing threshold adjustment. Our system-level simulation results demonstrate that the proposed framework boosts the areal capacity gain by approximately 4.42 times as much as the conventional approach.

INDEX TERMS Dynamic spectrum sharing, cellular network, listen-before-talk, hidden node problem, frequency reuse, areal capacity.

I. INTRODUCTION

To deal with growing traffic demands, many studies have focused on the dynamic spectrum sharing (DSS) environment, where a spectrum is shared by various wireless technologies or multiple mobile network operators (MNO) [1]. For example, long-term evolution (LTE) and new radio (NR) standards have been proposed to operate in the 5-GHz unlicensed band, and the concept of licensed shared access (LSA) is currently being developed with the aim of enabling cellular operators to access further spectral resources on a licensed shared basis [2]. One example is the 3.5-GHz Citizens Broadband Radio Service (CBRS) band under discussion [1]. As these trends eventually lead to extreme densification of various types of systems, a new DSS mechanism is needed to increase bandwidth efficiency even in extreme densification of multiple wireless technologies. In particular, since wireless traffic has been dominated by downlinks, e.g., file downloading and on-demand video streaming, we focus on the downlink DSS systems where each base station (or access point) dynamically occupies the channel in a distributed manner via a contending mechanism, e.g., listen-before-talk (LBT) or a carrier-sense multiple access with collision avoidance (CSMA/CA) protocol.

To maximize the areal capacity of the downlink DSS system, we should leverage the spatial frequency reuse gain as in the cellular system. In this type of the system, however, spectrum reuse is hindered by unpredictable co-channel interference (called the hidden node problem), which limits the areal capacity. Therefore, most previous related works have focused on dealing with the hidden node problem. Typical approaches include transmission-power control and carrier-sensing threshold (CST) control [3]–[5]. However, these approaches tend to clear an unnecessarily large area, thus significantly limiting the spatial frequency reuse gain.

Another approach to overcome the hidden node problem is to employ a modulation and coding scheme (MCS) of the

The associate editor coordinating the review of this manuscript and approving it for publication was Prabhat Kumar Upadhyay.

This work is licensed under a Creative Commons Attribution 4.0 License. For more information, see https://creativecommons.org/licenses/by/4.0/

user equipment (UE) based on the previous transmission history. For example, [6] proposes an open-loop link adaptation algorithm that determines MCS by observing the link layer acknowledgement (ACK) and the received signal strength indicator (RSSI). Since they allocate MCS based on the previous transmission history, base station (BS) cannot allocate optimal MCS corresponding to the instantaneous signal-to-interference-plus-noise ratio (SINR) of the UE, thus reducing the spectral efficiency. In [7], a closed-loop link adaptation algorithm for the downlink LAA system is proposed to consider the channel quality indicator (CQI) mismatch problem due to hidden nodes [7]. They utilize the distribution of past SINR reports to judge whether the reported SINR value is affected by the hidden nodes (called a collision event). Based on this information, they seek to select the best fixed MCS index that shows the highest throughput. As in [6], they cannot allocate an optimal MCS corresponding to the instantaneous SINR of the UE; this causes spectral-efficiency degradation, especially when BSs actively reuse the channel. In other words, they do not fully leverage the closed-loop link adaptation as in the cellular system.

As described, it is not possible to improve the spatial reuse gain in existing DSS systems while allocating the optimal MCS owing to the unpredictable nature of co-channel interference (i.e., hidden node problem). Fundamentally, this is attributed to the uncoordinated channel access mechanism of the current DSS systems. Specifically, since each BS performs LBT independently with no cooperation in existing DSS systems, the randomness in the BS patterns of occupying the channel leads to a serious hidden node problem, which incurs frequent CQI mismatch events.

In this work, we seek to develop a whole new framework, **group-wise DSS** framework, to overcome the fundamental limitation of the current DSS system. In this framework, all BSs are formed into groups of spatially adjacent BSs, and then a group-wise LBT procedure is introduced to achieve the full frequency reuse within each group. If a group succeeds in channel access, all BSs within that group concurrently begin data transmission, and then release the channel simultaneously. Here, we set an appropriate CST to mitigate the effect of a randomly generated out-of-group interference (OGI). This allows for keeping intra-group interference (IGI) generated within the group relatively stronger than the OGI, so that the CQI mismatch can be reduced significantly. Allowing for adjacent BSs to occupy the channel concurrently as much as possible without incurring a CQI mismatch results in a higher areal capacity than in the conventional approach. To implement this framework, we propose a joint optimization procedure by comprehensively designing the group-wise LBT protocol with the underlying BS grouping and CST control algorithms. Our system-level simulation based on the 3GPP-LAA evaluation methodology demonstrates that the proposed group-wise DSS framework boosts the areal capacity to approximately 4.42 times that of the conventional DSS approach.

The rest of the paper is organized as follows. Section II introduces the system model considered in this paper. Section III presents the proposed DSS framework, along with the group-wise LBT procedure as an essential element of our proposed concept. Section IV details the formulation of our design problem to determine a set of simultaneous transmission BSs that maximizes the given performance metric. Based on the corresponding grouping problem, we design the implementation framework for the group-wise LBT protocol. Subsequently, Section V presents the grouping algorithm and the CST control algorithm employed for the implementation framework. In Section VI, we demonstrate the feasibility and effectiveness of our proposed framework and algorithms through a system-level simulation. Finally, we conclude the paper in Section VII.

II. SYSTEM MODEL

The downlink DSS system can be coordinated or uncoordinated, depending on how all types of BSs are designed for coexistence. The uncoordinated DSS system mainly considers the situation in which each BS is independently operated as an individual (e.g., Wi-Fi) with no cooperative operation for all coexisting BSs. In the coordinated DSS system, all types of BSs are designed to be deployed under mutual cooperation between those managed by their own MNO. An example of the coordinated DSS system is 3GPP LAA and MulteFire specifications [8], which are designed to operate LTE systems in unlicensed bands in a standalone or non-standalone manner while maintaining all key features of the cellular systems, such as seamless handover, physical cell identification (PCI) planning, interference management by self-organizing network (SON), and coordinated multipoint transmission (CoMP). In other words, a set of BSs managed by each MNO are designed to enhance the system throughput by their mutual cooperation over their own channel occupancy in the coordinated DSS system. In this paper, we focus on a downlink coordinated DSS system, especially for coexistence in a common spectrum, which is expected to be of high practical relevance in the near future [1]. Thus, we basically follow the system model of the 3GPP LAA system. Specifically, for coexistence between the BSs in the shared spectrum, we consider the LBT protocol with an exponential back-off mechanism [9], [10]. All BSs in the system are synchronized to the subframe boundary to inherit the cellular operation in LTE. We assume that the omnidirectional antenna is employed. In addition, the BSs can be managed by a central network entity as in the existing cellular systems.

By default, LAA adopts adaptive modulation and coding (AMC) to allocate an MCS that corresponds to the instantaneous SINR measured by UE. Fig. 1 illustrates a link adaptation procedure with AMC [7]. The BS first transmits a cell-specific reference signal (CRS) in every downlink subframe, which allows measuring of SINR in each UE. Once CQI is determined upon the measured SINR, it is reported to the BS through an uplink control channel. Based on the

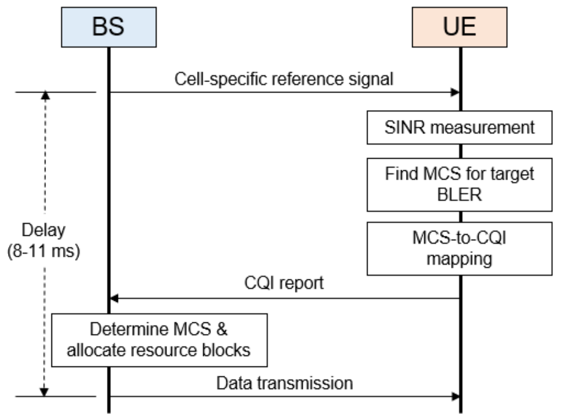

FIGURE 1. **Link adaptation procedure with adaptive modulation and coding (AMC) [7].**

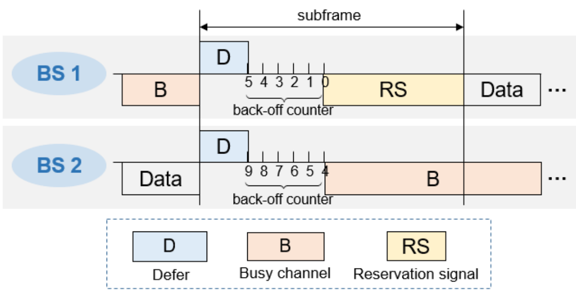

FIGURE 2. **LBT procedure for coordinated DSS system.**

CQI report, BS assigns the resource for the next downlink transmission with the corresponding MCS. In general, the delay associated with the CRS transmission to the BSs receiving the CQI is normally in the range of 8−11 ms as illustrated in Fig. 1 [11].

Fig. 2 illustrates a typical LBT procedure for the coordinated DSS system. Basically, LBT in the 3GPP LAA system is designed in the same way as CSMA/CA for fair-coexistence with IEEE 802.11 Wireless Local Area Network (Wi-Fi). Specifically, before the BS generates a back-off count, it performs a Defer operation over consecutive clear channel assessment (CCA) slots. The CCA slot is considered idle if a power level measured by the BS within the CCA slot duration is below the CST. Otherwise, it is considered busy, and then the BS persists to sense the channel until it becomes idle for the duration of Defer. This is essential for fair coexistence, e.g., providing transmission opportunity for short frames. If the BS still finds the channel idle after the duration of Defer, it generates a back-off count, which is a random number chosen within a back-off window size. The back-off count is decremented as long as the channel is sensed idle, frozen when the channel is sensed busy, and reactivated when the channel is sensed idle for the duration of Defer. When the back-off count reaches zero, the BS can occupy the channel up to the maximum channel-occupancy time (MCOT) [10]. It is noteworthy that an exponential back-off mechanism is employed to adjust the contention window size, e.g., based on the ACK/NACK ratio. Once a channel is captured by the BS, a dummy signal, referred to as a reservation signal (RS), must be transmitted until the end of the current subframe to ensure that the start of all transmissions is aligned by the subframe boundary.

III. GROUP-WISE DYNAMIC SPECTRUM SHARING (DSS)

As aforementioned, an uncoordinated DSS system mainly considers the situation in which each BS is independently operated as an individual. This means that each BS must go through its own channel access procedure, e.g., CSMA/CA. As MCOT is limited to the unit of milliseconds for fairness between them, the sources of the hidden node interference are changed randomly at the same time scale, implying that a closed-loop feedback mechanism might not be reliable for link adaptation. Meanwhile, for a stable CQI report of the UE, we assume that the UE can reliably report the CQI through a separate uplink channel or resource as in LAA. Of course, a CST can be sensitively set to avoid the hidden node interference, yet reduce the spatial reuse efficiency. Therefore, owing to the hidden node problem, only an open loop-based link adaptation, e.g., auto rate fallback mechanism [6], is implemented in the uncoordinated DSS system, relying on transmission failure experience. Meanwhile, closed-loop-based link adaptation is a useful means of allowing full frequency reuse in conventional cellular systems, e.g., LTE and NR systems. Although coordinated DSS systems can inherit the full frequency reuse operation as in cellular systems, they might suffer from frequent CQI mismatch as a result of the LBT protocol for fair coexistence among uncoordinated DSS systems.

Each BS independently performs LBT with no cooperation in the current DSS systems. Thus, their areal capacity is limited by the hidden node problem, especially when the BS becomes denser [12]. This is in contrast to the cellular systems operating in the licensed band, e.g., the 4G LTE and 5G NR systems, which can increase areal capacity without limitation by densifying the BSs. The full frequency reusability in the licensed bands is enabled by reliable and flexible link adaptation over the shared frequency resources without resorting to unnecessarily large reuse distances. In other words, as a result of the static co-channel interference between BSs, the interference level experienced by the UE is highly time-correlated unlike systems operating in unlicensed bands. Thus, regardless of how aggressively the BSs reuse frequency resources—even with a few millisecond delays in the CQI report—link adaptation works well with closed-loop feedback for AMC. In the following subsections, we seek to develop a whole new framework to integrate a similar spatial reuse capability of the cellular system into the downlink coordinated DSS system.

Fig. 3 presents illustrative examples for the existing DSS and group-wise DSS approaches for comparison. Therein, channel occupation patterns along a timeline are illustrated with a snapshot for a spatial-reuse situation. Additionally, the effect of the hidden nodes on the signal-to-interference

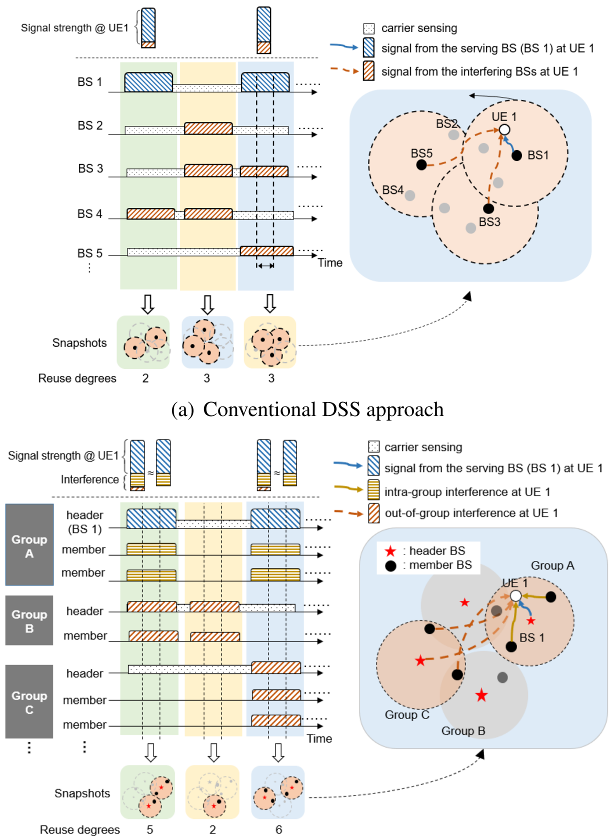

(a) Conventional DSS approach

(b) Group-wise DSS approach

FIGURE 3. Illustrative examples: conventional vs. group-wise DSS approach.

ratio (SIR) is shown for a typical UE 1 associated with BS 1 in the current interference-limited environment. As illustrated in Fig. 3(a), an individual BS in the existing DSS approach performs LBT for its own channel occupation while clearing up the nearby BSs. Owing to the individual channel occupation, the SIR level of UE 1 varied unpredictably, causing unreliable link adaptation. The SIR level can be stabilized by setting the CST sufficiently small to clear up the potential hidden nodes, i.e., increasing the carrier-sensing range (CSR). The illustrated snapshot shows three BSs transmitting simultaneously in the given area.

Meanwhile, Fig. 3(b) illustrates the proposed group-wise LBT process, in which all member BSs in a group transmit simultaneously with the header BS. Since stronger IGI is experienced in a fixed pattern owing to the group-wise simultaneous transmission, UE 1 maintains a rather stable SIR level against the OGI, allowing for reliable link adaptation, as in the cellular systems. As illustrated by the snapshot in Fig. 3(b), more BSs are allowed to occupy the channel concurrently in the same area than in the case in Fig. 3(a).

A. GROUP-WISE DSS: PRINCIPLE

The hidden node problem in the existing DSS system limits the system efficiency because of the unpredictable nature of co-channel interference. Herein, we intend to invent a means of dealing with the hidden node problem without resorting to a large reuse distance. It clusters adjacent BSs into BS groups, each of which performs its own LBT protocol. If a group succeeds in LBT, then all BSs in the group concurrently transmit data and release the channel, allowing for full frequency reuse within the group. As all grouped BSs must concurrently transmit data, we assume that all candidate BSs to be grouped are in a full-buffer state. In each group, one BS is designated as a header BS, which performs LBT on behalf of the other member BSs in the same group. If the header BS succeeds in occupying the channel after performing LBT, then all member BSs in the group occupy the channel without going through the LBT procedure. In this particular group-wise approach under consideration, the random effect of OGI on the received SINR can be reduced by setting an appropriate CST.

B. GROUP-WISE LBT PROTOCOL

To implement the aforementioned concept, a group-wise channel access procedure is required to enable all BSs in the same group to concurrently transmit data. When each BS in the group performs its own LBT protocol independently, it is highly inefficient for all BSs in the group to concurrently occupy the channel, since they have to wait until all become active and contend to win. In the proposed group-wise DSS framework, however, all member BSs in the group occupy the channel without the LBT procedure once its header BS wins the channel contention. Since the header BS eliminates undesired nodes that contend for their own individual channel access, the CQI mismatch can be reduced by avoiding unnecessary MAC collision events. In other words, once all BSs are clustered into multiple groups, the CQI mismatch effect can be reduced in two aspects: (1) CST control to deal with random OGIs due to hidden nodes, and (2) MAC collision reduction by designating a header BS in each group. For (1), a sufficiently wide area must be cleared up to prevent the member BSs from experiencing strong OGI. In other words, CST must be set sufficiently small enough to neglect the OGI for the given BS grouping solution. In the next section, we present a specific grouping algorithm to maximize the areal capacity in the DSS environment.

Fig. 4(a) illustrates the detailed operation of the proposed channel access scheme. Once BS 1 (header BS of Group A) succeeds in LBT, it initiates a group-triggering signal (GTS) of Group A (denoted as GTS(A)) to indicate that it has occupied the channel. Once the GTS(A) is reached by the member BSs of Group A, they transmit GTS(A) to occupy the channel simultaneously. To ensure that data transmission is aligned with a subframe boundary for full frequency reuse, the header BS and its member BSs transmit GTS(A) simultaneously until the end of the current subframe. However, if the header BS finds that the channel is busy because of OGI, e.g., sensing the GTS from another group, the back-off count decrement is stopped (e.g., BS 3 of Group B in Fig. 4(a)). Meanwhile, BS 4—which is a member BS of Group B—waits to detect the

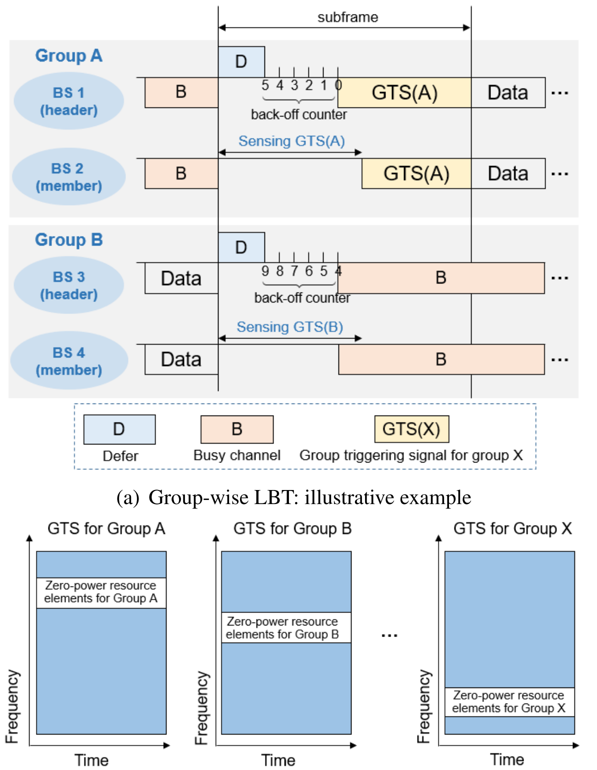

(a) Group-wise LBT: illustrative example

(b) Group triggering signaling (GTS) with zero-power resource elements: design illustration

FIGURE 4. Group-wise LBT protocol: (a) Illustrative example (b) Group triggering signal (GTS).

GTS of Group B, denoted as GTS(B), but finds the channel busy because of GTS(A).

To implement this procedure, the member BSs must be able to recognize the GTS transmitted from their group header BS. As an implementation method, the GTS for each group can be distinguished by allocating zero-power frequency resources at different positions for each group, as shown in Fig. 4(b). Alternatively, the GTS can be implemented by sending an explicit message containing the group identification (ID) or by assigning an orthogonal sequence for each group [13]. Herein, since the GTS is designed to transmit the reservation signal in a specific form, there is no additional resource overhead associated with the GTS transmission in the group-wise LBT. Thus, its complexity is the same as that of the existing LBT scheme in 3GPP. In conclusion, the group-wise LBT can coexist with various types of nodes through the LBT procedure with low overhead.

IV. IMPLEMENTATION FRAMEWORK FOR GROUP-WISE LBT PROTOCOL

It has been shown by the Poisson point process (PPP)-based analysis in [14] that areal capacity can be increased with numerous BSs transmitting simultaneously. However, it holds only when the Shannon capacity can be achieved without losing capacity because of CQI mismatch for each UE. This is also true for the proposed group-wise LBT, in which the CQI mismatch can be reduced by the CST control mechanism. Then, our design objective is to maximize the number of BS groups occupying the channel simultaneously, defined as the degree of frequency reuse (*"reuse degree"*), without compromising the theoretically warranted capacity. As illustrated in Fig. 3(b), its reuse degree varies over time in the group-wise LBT protocol. This section details the formulation of the problem to determine reuse groups that maximize the average reuse degree for a given BS topology. Based on the formulated problem, we present the key steps for implementing the group-wise LBT protocol, including the grouping and CST control procedure.

A. PROBLEM FORMULATION

The CSR of a header BS must be maintained sufficiently large to neglect the OGI subject to the given IGI strength. This implies that CSR must be somehow controlled by the CST, establishing a one-to-one relationship between the CSR and CST. Toward this end, we first assume that all groups employ the same value of CST. Then, carrier sensing is based on the interference strength of each BS, rather than the total interference, so that the CSR is inversely proportional to the CST. Note that this operation can be enabled by CRS detection (or preamble detection as in Wi-Fi specification). Furthermore, we assume that each group has the same average channel access probability. This assumption is acceptable provided each group employs the same LBT parameters. Then, the average reuse degree can be expressed as a product of the average number of simultaneous transmission groups and the average number of BSs per group. In the sequel, we formulate a BS grouping problem to capture a trade-off between them.

More specifically, let $\mathcal{B}$ denote a set of BSs to be grouped with $|\mathcal{B}| = N_{\mathcal{B}}$. To represent the BS topology, we introduce a similarity matrix, denoted by $\mathbf{D} = [d_{ij}]_{N_{\mathcal{B}} \times N_{\mathcal{B}}}$, in which each element d_{ij} is the physical distance between BS i and BS j for $\forall i \neq j$, and d_{ii} is zero for $\forall i \in \mathcal{B}$. In a practical scenario, the minimum received signal strength (RSS) that can detect OGI at the header BS is limited owing to various factors, e.g., receiver sensitivity and transmission power. In other words, the maximum CSR of a header BS can be limited, and thus we define the grouping boundary as the maximum distance between the header BS and a member BS, denoted by d_{limit}. If the distance between BS i and BS j is more than d_{limit}, we set $d_{limit} = \infty$. Subsequently, let $\mathbf{X} = [x_{ij}]_{N_{\mathcal{B}} \times N_{\mathcal{B}}}$ be a group assignment matrix, where the non-diagonal elements $x_{ij} \in \{0, 1\}$ indicate that BS j is a header BS of the BS i if $x_{ij} = 1$, where the diagonal elements $x_{jj} \in \{0, 1\}$ indicate that BS j is the header BS, i.e.,

$$x_{ij} = \begin{cases} 1 & \text{if BS } j \text{ is a header of BS } i, \\ 0 & \text{otherwise,} \end{cases} \quad \forall i \neq j,$$

$$x_{jj} = \begin{cases} 1 & \text{if BS } j \text{ is a header BS,} \\ 0 & \text{otherwise,} \end{cases} \quad \forall j.$$

Spatial reuse among the different reuse groups becomes aggressive with the CST value. Thus, to maximize the reuse degree in the group-wise LBT protocol, we should set the highest possible CST value that satisfies the target transmission failure probability (TFP). Therefore, given $\mathbf{X}$ and $\mathbf{D}$, we define a safe-CST of the group-wise LBT (equivalently, safe-CSR defined by the safe-CST), denoted by $CST\,(\mathbf{X}, \mathbf{D})$, as the maximum CST value while satisfying the target TFP. Let $\rho_g\,(CST\,(\mathbf{X}, \mathbf{D}))$ denote the reuse degree of the groups, which corresponds to the average number of groups occupying the channel simultaneously when using $CST\,(\mathbf{X}, \mathbf{D})$. Since the number of groups follows $\sum_{j \in \mathcal{B}} x_{jj} \triangleq k$, the average number of BSs per group is given by $N_{\mathcal{B}}/k$. Our average reuse degree maximization problem for the proposed group-wise LBT protocol is the determination of a set of header BSs and their member BSs simultaneously. This is formulated for the given BS topology $\mathbf{D}$ as follows:

$$\max_{\mathbf{X}} \rho_g\,(CST\,(\mathbf{X}, \mathbf{D})) \cdot N_{\mathcal{B}}/k \tag{1}$$

$$\text{s.t.,} \sum_{j \in \mathcal{B}} x_{ij} = 1, \quad \forall i \in \mathcal{B}, \tag{2}$$

$$\sum_{\forall i \neq j} x_{ij} > x_{jj} - 1, \quad \forall j \in \mathcal{B}, \tag{3}$$

$$\sum\nolimits_{j \in \mathcal{B}} x_{jj} = k, \tag{4}$$

$$x_{ij} \leq x_{jj}, \quad \forall i, j \in \mathcal{B}, \tag{5}$$

$$x_{ij} \in \{0, 1\}, \quad \forall i, j \in \mathcal{B}. \tag{6}$$

Here, the first constraint in (2) dictates that each member BS chooses its own single header BS. The constraint in (3) implies that at least one member BS should exist per group. The constraint in (4) indicates that the number of groups is k. The constraint in (5) dictates that BS j must be a header BS if there exists a BS i selecting BS j as its header BS. As it is not straightforward to find an explicit expression for $CST\,(\mathbf{X}, \mathbf{D})$ in (1), we resort to solving its sub-problem by fixing the number of groups; this is detailed in the following subsection.

B. SUBOPTIMAL SOLUTION APPROACH

When k is fixed in (1), the average number of BSs per group, $N_{\mathcal{B}}/k$, is also fixed. Thus, the reuse degree of the group, $\rho_g\,(CST\,(\mathbf{X}, \mathbf{D}))$, is the objective function in (1). Then, it is maximized by increasing the safe-CST value, $CST\,(\mathbf{X}, \mathbf{D})$. In other words, we aim to determine a grouping solution X that maximizes $CST\,(\mathbf{X}, \mathbf{D})$. Once the IGI is determined by X, the CST can be controlled to set an acceptable level of the OGI. This implies that the IGI and OGI must be balanced by the CST value to limit the CQI mismatch to the desired level. In an interference-limited environment, let us focus on the UE associated with the BS using the group-wise LBT protocol. Given its power S received from the serving BSs, let I_{IGI} and I_{OGI} be the signal strength of the IGI and OGI in the UE, respectively. Provided $I_{IGI} \gg I_{OGI}$, i.e., the influence of the randomly generated OGI through the group-wise LBT protocol can be ignored, the UE reports the CQI value corresponding to the $10\log_{10}\,(S/I_{IGI})$ dB to the serving BS.

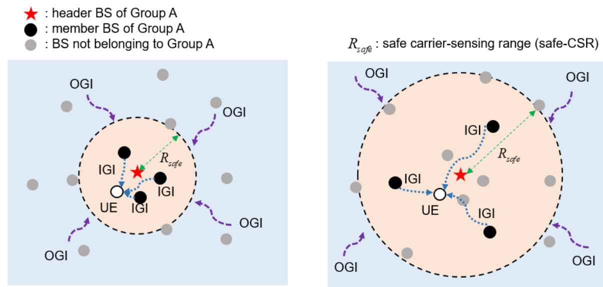

(a) Small safe-CSR (b) Large safe-CSR

FIGURE 5. Comparison of BS grouping for spatial reuse with the different values of safe-CSR under the fixed number of BSs in each group ($N_{\mathcal{B}}/k = 4$): (a) Small safe-CSR, (b) Large safe-CSR.

Then, its MCS level, denoted as γ, is assigned accordingly. Let σ_γ be the required minimum SIR for the MCS level γ. To avoid a CQI mismatch subject to OGI, the SIR reduction by OGI must be less than $10\log_{10}\,(S/I_{IGI}) - \sigma_\gamma \triangleq \Delta\sigma_\gamma$ dB. Then, the following inequality must be satisfied for I_{IGI} and I_{OGI}:

$$10\log_{10}\left(\frac{S}{I_{IGI}}\right) - 10\log_{10}\left(\frac{S}{I_{IGI} + I_{OGI}}\right) = 10\log_{10}\left(1 + \frac{I_{OGI}}{I_{IGI}}\right) \leq \Delta\sigma_\gamma. \tag{7}$$

Equation (7) implies that the CQI mismatch is governed by the ratio between the IGI and OGI regardless of the signal strength from a serving BS. In other words, the strength of the IGI can be increased by grouping the BSs more densely, which subsequently reduces the safe-CSR (i.e., increases the safe-CST value) to realize a greater reuse degree among the groups. Fig. 5 illustrates how the reuse degree is governed by the different values of safe-CSR for the fixed number of BSs in each group. It intends to illustrates how the BSs must be grouped by adjusting the safe-CSR for the given number of BSs in each group, e.g., four BSs in each group ($N_{\mathcal{B}}/k = 4$). In order to increase the reuse degree in this example, the safe-CSR must be reduced to get all four BSs as close as possible in a group. In that case, the multiple groups would be reused throughout the given region as in Fig. 5(a). Meanwhile, if the safe-CSR is too large to induce sparse BS's in a group, e.g., as in Fig. 5(b), the many groups in the same region cannot be reused simultaneously, reducing the reuse degree among the groups. Compared between two cases in Fig. 5(a) and (b), it is clearly shown that all BSs in the same group must be clustered as close as possible to each other, leading to more spatial reuse degrees while maintaining $I_{IGI} \gg I_{OGI}$. Furthermore, the most central BS in a group must be designated as a header BS. When the other BS is selected as a header BS, the CSR of the header BS must be enlarged to protect all member BSs from the OGI, reducing the reuse degree. This implies that our BS grouping problem can be reformulated to minimize the sum of the squared Euclidean distances between the header BS and its member BS for k groups. More specifically, it leads to the following

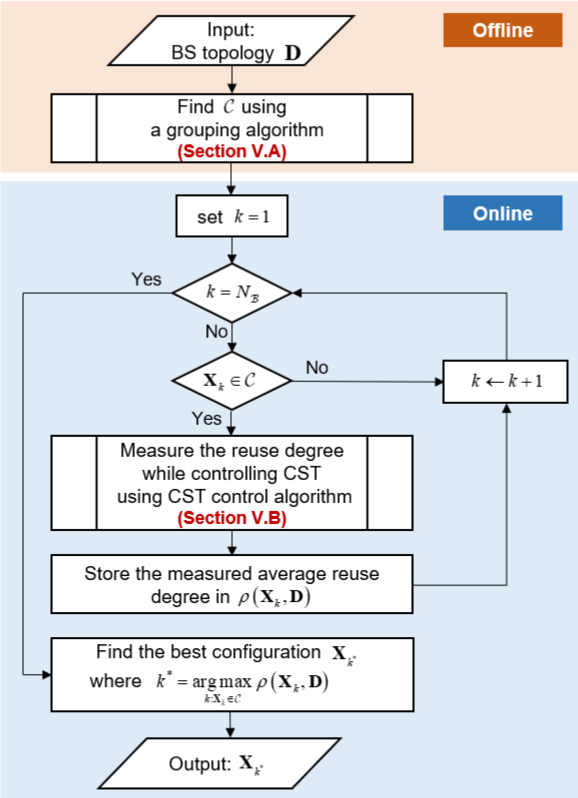

FIGURE 6. Implementation framework for group-wise LBT protocol.

optimization problem for a given $\mathbf{D}$:

$$\min_{\mathbf{X}} \sum_{i \in \mathcal{B}} \sum_{j \in \mathcal{B}} x_{ij} d_{ij}^2 \tag{8}$$

with the same constraints as in (2)-(6). As (8) is NP-hard, we discuss a heuristic algorithm, referred to as a DSS-grouping algorithm, in the next section.

Once BS grouping is completed for the given number of groups, we can resort to an exhaustive search for overall optimization, as presented in Fig. 6, which shows the overall implementation framework for group-wise LBT protocol. For the given BS topology $\mathbf{D}$, let $\mathbf{X}_k$ denote the grouping configuration derived by a heuristic algorithm for (8) with k groups. Note that a feasible solution to (8) may not exist, depending on BS topology and the constraints; for example, the constraint (3) is violated for $N_{\mathcal{B}} = 10$ and $k = 8$. Therefore, we construct a set of $\{\mathbf{X}_k\}_{k=1}^{N_{\mathcal{B}}}$ which satisfies (8), denoted by $\mathcal{C}$. Since $\mathcal{C}$ can be constructed for the given BS topology $\mathbf{D}$, this procedure works offline.

Subsequently, we measure the average reuse degree corresponding to $\mathbf{X}_k$ while controlling CST by another algorithm, referred to as the CST control algorithm in the following section. The average reuse degree, denoted by $\rho(\mathbf{X}_k, \mathbf{D})$, is measured by taking the time average for the number of concurrently transmitting BSs within the subframe over the given observation time. Finally, we conduct an exhaustive search to find the best configuration $\mathbf{X}_{k^*}$ such that

$$k^* = \arg\max_{k:\mathbf{X}_k \in \mathcal{C}} \rho(\mathbf{X}_k, \mathbf{D}). \tag{9}$$

Note that this optimization procedure works online because the required information (e.g., TFP and reuse degree) is provided to the algorithm over time.

V. ALGORITHM DESIGN

The optimization procedure in Section IV (also specified by the flow chart in Fig. 6) requires two separate algorithms: one proposed for BS grouping by constructing $\mathbf{X}$ and the other proposed for CST control that determines $CST(\mathbf{X}_k, \mathbf{D})$ for each $\mathbf{X}_k \in \mathcal{C}$. These algorithms are detailed in this section.

A. DSS-GROUPING ALGORITHM

We use a heuristic algorithm to find $\{\mathbf{X}_k\}_{k=1}^{N_{\mathcal{B}}}$ because of the NP-hardness of (8). We note that (8) is similar to a typical clustering problem, which clusters adjacent points into k disjoint groups such that their squared Euclidean distances between all centers and their associated nodes are minimized. The only difference from a standard clustering problem is that (8) involves some constraints. Therefore, existing algorithms, e.g., k-means or k-medoids algorithm, can be employed while screening the solutions subject to the underlying constraints.

The k-medoids algorithm attempts to minimize the distance between points labeled as in a group, and a medoid is designated as the center of that group. In the k-medoids algorithm, the medoid is chosen for each group in each iteration rather than calculating the mean of the points in each group [15], [16]. Since we want to find the medoids in each group (i.e., a header BS) rather than the mean of the points, it is intuitively more suitable to find the solution to (8) using the k-medoids algorithm rather than the k-means algorithm. Therefore, the k-medoids algorithm is employed to derive the solution $\mathbf{X}_k$ for each $k = 1, 2, \cdots, N_{\mathcal{B}}$.

Recall that we set $d_{ij} = \infty$ if the distance between the header BS and its member BS is more than d_{limit}. Moreover, the solution derived from the k-medoids algorithm may not satisfy (3). Therefore, when we construct the set of available group configurations $\mathcal{C}$, we screen out the solution $\mathbf{X}_k$ which yields ∞ in (8) and does not satisfy (3). The detailed procedure for the DSS-grouping algorithm is now specified as **Algorithm 1**. Fig. 7 illustrates all its iterative steps with a simple example.

In **Algorithm 1**, we randomly select the header BSs at the initialization step. Then, the k-medoids algorithm used in **Algorithm 1** finds a solution in a greedy manner, which would ends up at a local optimum. Since our purpose is to verify the effectiveness of the group-wise LBT and its implementation framework, more advanced algorithms can be designed to improve its performance with the various other approaches, which is beyond the scope of this paper.

Algorithm 1 DSS-Grouping Algorithm

Set $\mathcal{C} = \varnothing$
for $k = 1, 2, \cdots, N_{\mathcal{B}}$ **do**
  Step 1 (Initialization):
  1.1. Choose k BSs at random to be the initial header BSs;
  1.2. Assign each member BS to the nearest header BS;
  Step 2 (Update header BSs):
  2.1. Find a new header BS in each group, which is the object minimizing the total distance from the member BSs in its group;
  2.2. Update the current header BS in each group by replacing it with the new header BS;
  Step 3 (Assign member BSs to header BSs):
  3.1. Assign each object to the nearest header BS and obtain the grouping configuration;
  3.2. Repeat Step 2 and 3 until all header BSs become fixed;
  3.3. If all header BSs become fixed, save the current group configuration on $\mathbf{X}_k$;
  Step 4: (Screen solution):
  4.1. If $\mathbf{X}_k$ yields a finite output in (8) and satisfies (3), $\mathcal{C} = \mathcal{C} \bigcup \{\mathbf{X}_k\}$
end

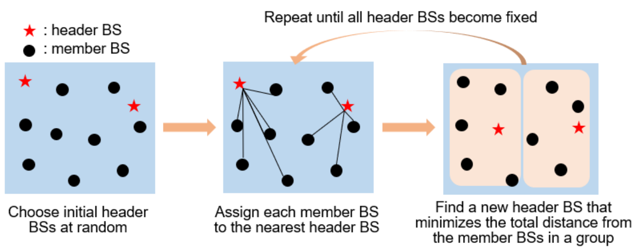

FIGURE 7. Illustrative example of k-medoids algorithm.

B. CST CONTROL ALGORITHM (CSTA)

As mentioned above, spatial reuse among the groups increases with the CST. Therefore, we seek to find the highest CST value that satisfies the target TFP for the given grouping solution by **Algorithm 1** (i.e., $CST\,(\mathbf{X}_k, \mathbf{D})$). TFP can be reduced by decreasing CST, since OGI is proportional to CST. However, even if the CST is fixed, TFP may still vary over time due to the network dynamics, e.g., MAC collision, and channel fading, in practice. Also, the complexity of the network dynamics renders it difficult to determine a network evolution model in advance [17]. In order to maintain the TFP performance within the required level, CST must be controlled in the varying environment, yet at its highest possible threshold. Toward this end, we design the Q-learning algorithm for group-wise LBT that can control the CST value in adaptation to the dynamically changing wireless network environment [9].

The Q-learning algorithm, as the most widely used model-free learning algorithm, consists of the following three elements: 1) states; 2) actions; and 3) rewards (costs), and the goal of the Q-learning algorithm is to maximize the total reward [9]. Let us consider a sequence which represents the decision epochs, denoted by $\mathcal{T} = \{1, 2, \ldots, N_{\mathcal{T}}\}$. Herein, $N_{\mathcal{T}}$ is the maximum number of decision epochs and the duration between the decision epoch is a constant value λ (e.g., $\lambda = 100$ ms). s_t and a_t denote the state and the action chosen at the decision epoch $t \in T$, respectively. At the decision epoch $t \in \mathcal{T}$, the learner selects an action a_t and observes a reward $r\,(s_t, a_t)$, and enters a new state s_{t+1}. Based on the received reward $r\,(s_t, a_t)$, the Q-value $Q\,(s_t, a_t)$, which represents the quality of action a_t selected for state s_t, is updated as follows:

$$Q\,(s_t, a_t) \leftarrow (1-\alpha)\, Q\,(s_t, a_t) + \alpha \left(r\,(s_t, a_t) + \gamma \max_{a} Q\,(s_{t+1}, a) \right) \quad (10)$$

where α is the learning rate $(0 \leq \alpha \leq 1)$ and γ is the discount factor $(0 \leq \gamma \leq 1)$. In the group-wise LBT protocol, our design objective is to determine the maximum CST that satisfies the target TFP, denoted by β_{TFP}. In the sequel, we define states, actions, and rewards in terms of the TFP and CST values for our design.

Let $\mathcal{P}$ denote a set of possible CST values. Considering $N_{\mathcal{P}}$ possible CST values, it is constructed as

$$\mathcal{P} = \left\{ CST_1, CST_2, \cdots, CST_{N_{\mathcal{P}}} \right\}$$

where CST_i is the i-th state given by a CST value (dBm) and $CST_i > CST_{i+1}$. Let $p_t \in \mathcal{P}$ denote a state for CST that is applied over $(t-1, t]$. In this algorithm, for stable operation of the group-wise LBT protocol, we fix the maximum and minimum CST values, denoted by $CST_{\max}$ and $CST_{\min}$, respectively. Therefore, $CST_1 \leq CST_{\max}$ and $CST_{N_{\mathcal{P}}} \geq CST_{\min}$. Herein, based on the minimum detection strength of LTE CRS [18], we set $CST_{\max} = -53$ dBm and $CST_{\min} = -91$ dBm. Note that CSR can be adjusted more finely with increasing $N_{\mathcal{P}}$. Too many states might be involved with enormous training overhead without significant performance improvement. In order to induce a meaningful change in TFP by a state change, however, the number of states in P must be set large enough to increase or decrease CSR uniformly. For example, if a control interval of the CSR is about 30 m within the minimum and maximum range of CST, $N_{\mathcal{P}} = 12$ warrants an acceptable amount of training overhead without compromising its average throughput performance. More specifically, consider the NLoS path-loss in urban micro (UMi) scenario, which is modeled as

$$l_{\mathrm{NLoS}}(\mathrm{dB}) = 36.7\log_{10} d + 22.7 + 26\log_{10} 2.4 \quad (11)$$

where d is the 3D distance between the transmitter and receiver [19]. Assuming the BS transmit power of 30 dBm under the UMi NLoS path-loss model in (11), $\mathcal{P}$ can be set as follows:

$$\mathcal{P} = \left\{ \begin{array}{l} -53, -63, -69, -74, -77, -80, \\ -82.5, -85, -87, -88.5, -90, -91 \end{array} \right\}. \quad (12)$$

Meanwhile, consider two states, 0 and 1, to indicate whether the observed TFP satisfies the target TFP with the current value of CST. Let $\mathcal{F}$ denote the set of these two states, i.e., $\mathcal{F} = \{0, 1\}$. In the course of running the algorithm, TFP must be measured online. Let m_{t+1} denote the instantaneous TFP measured when CST p_{t+1} is applied over $(t, t+1]$. It can be measured by counting the number of transmission successes and failures. Meanwhile, let $\overline{F}_t(CST_i)$ denote the average TFP for each CST_i at decision epoch t. If $p_{t+1} = CST_i$, $\overline{F}_{t+1}(CST_i)$ will be updated by the following exponential moving average (EMA):

$$\overline{F}_{t+1}(CST_i) = \begin{cases} (1-\omega)\overline{F}_t(CST_i) & \\ +\omega m_{t+1} & \text{if} p_{t+1} = CST_i, \\ \overline{F}_t(CST_i) & \text{if } p_{t+1} \neq CST_i, \end{cases} \quad (13)$$

where ω is a discount factor for the EMA. Herein, initial value of $\overline{F}_{t+1}(CST_i)$ is set to the very first instantaneous transmission failure probability when CST_i is applied. Let $f_t \in \mathcal{F}$ denote a state to indicate whether $\overline{F}_t(p_t) < \beta_{TFP}$ at decision epoch t, i.e., $f_t = 0$ if $\overline{F}_t(p_t) < \beta_{TFP}$ and $f_t = 1$ otherwise. Given two sets, $\mathcal{P}$ and $\mathcal{F}$, state space $\mathcal{S}$ can defined as the Cartesian product of $\mathcal{P}$ and $\mathcal{F}$, i.e., $\mathcal{S} = \mathcal{P} \times \mathcal{F}$. At decision epoch t, its state is denoted as $s_t \in \mathcal{S}$, where $s_t = [p_t, f_t]$.

In a given state $p_t = CST_i$, we seek to determine the CST value to be employed during $(t, t+1]$, i.e., p_{t+1}. Among $N_{\mathcal{P}}$ possible states, we consider only one-step transitions between two neighbor CST values [20]. Limiting to one-step transitions, action space can be significantly reduced for the given state. In other words, action space varies with the current state. Let $\mathcal{A}_t$ denote action space at decision epoch t, which is given by a finite set of available actions to be selected when the current state is p_t. Following our one-step transition constraint, then the action set $\mathcal{A}_t$ is given as

$$\mathcal{A}_t = \begin{cases} \{CST_1, CST_2\} & \text{if } p_t = CST_1, \\ \{CST_{N_{\mathcal{P}}-1}, CST_{N_{\mathcal{P}}}\} & \text{if } p_t = CST_{N_{\mathcal{P}}}, \\ \{CST_{i-1}, CST_i, CST_{i+1}\} & \text{otherwise}. \end{cases} \quad (14)$$

Given a state $s_t = [p_t, f_t]$, action at decision epoch t, denoted as a_t, will be selected from the action set $\mathcal{A}_t$, i.e., $a_t \in \mathcal{A}_t$.

As mentioned above, we seek to maintain the highest CST value that satisfies the target TFP β_{TFP}. Therefore, we design a reward function, $r(s_t, a_t)$, which depends on whether $\overline{F_{t+1}}(p_{t+1}) < \beta_{TFP}$ is met or not. More specifically, if $\overline{F_{t+1}}(p_{t+1}) < \beta_{TFP}$, we give a positive reward, which is proportional to the CST p_{t+1} while making it as high as possible, i.e., $r(s_t, a_t) \leftarrow p_{t+1} - CST_{N_{\mathcal{P}}}$. However, if $\overline{F_{t+1}}(p_{t+1}) \geq \beta_{TFP}$, we give a negative reward in proportion to the CST p_{t+1}, i.e., $r(s_t, a_t) \leftarrow -\left(p_{t+1} - CST_{N_{\mathcal{P}}}\right)$, which can ensure that TFP is reduced.

Finally, to select the action at the decision epoch t, we use the ε-greedy policy, which is a combination of exploitation and exploration method as follows [9]:

$$a_t = \begin{cases} \arg\max_{a \in \mathcal{A}(p_t)} Q(s_t, a) & \text{with probability } 1\text{-}\varepsilon \\ & \text{(exploitation)}, \\ \text{random}\{a, a \in \mathcal{A}(p_t)\} & \text{with probability} \varepsilon \\ & \text{(exploration)}, \end{cases} \quad (15)$$

where ε is the exploration probability. Meanwhile, in the early stage of Q-learning, the performance of reuse degree may be distorted because the Q-values are not sufficiently updated. Thus, we need to wait until the Q-values are updated enough. Let N_{tr} be the number of decision epochs for training. Before Q-learning begins, all Q-values are initialized to 0. We do not consider the reuse degree during the training period, i.e., $t = 1 : N_{tr}$, and the reuse degree during $t = N_{tr} : N_{\mathcal{T}}$ is recorded on $\rho(\mathbf{X}_k, \mathbf{D})$.

VI. SYSTEM-LEVEL SIMULATION AND PERFORMANCE ANALYSIS

In this section, we focus on the performance evaluation of the areal capacity gain of the proposed and conventional schemes. Herein, the proposed scheme refers to the group-wise LBT that employs the DSS-grouping and CST control algorithms designed in this study, and the conventional scheme is the existing channel access mechanism in which each BS independently performs LBT with n cooperation. First, we present the system-level simulation scenario, including the simulation environment and system model. Then, our simulation results are presented to demonstrate the reuse gain of the proposed scheme over the conventional schemes.

A. SIMULATION SCENARIO

We adopted the LAA system for our DSS system model under consideration. The system-level simulator (SLS) developed using the C ++ language is implemented according to the 3GPP LAA evaluation methodology specified in [19]. This methodology corresponds to one developed to evaluate the system-level performance of the contributions to the 3GPP-LAA standardization process, which underwent various calibration procedures to verify its validity [21].

To verify the proposed scheme in the actual environment, we consider an environment in which 100 BSs are uniformly distributed in a square space. As aforementioned, the performance of the proposed scheme varies with the density of the BSs. Therefore, with the number of fixed BSs, we vary the area of the square to change the density of the BSs to limit the complexity of the simulation. Let d_{BS} denote the average distance between adjacent BSs. Then, we set up a square with an area of $10d_{BS}$x$10d_{BS}$, and the performance of the proposed and conventional scheme are observed for varying d_{BS} values. Notably, since 100 BSs are dropped in a square with an area of $10d_{BS}$x$10d_{BS}$, BSs are densely distributed as d_{BS} decreases. UEs are uniformly distributed in the square area and they associate with the BS that has the highest RSS.

TABLE 1. Simulation models and parameters.

Models and parameters		Value
Channel model	Carrier frequency	2.4 GHz
	Antenna configuration	2D omni-directional, 1Tx-2Rx (cross-polarized)
	Spatial channel model	ITU urban micro
	UE speed	3 km/h
System model	System bandwidth	20 MHz
	Number of component carriers	1
	Tx power	30 dBm
	Number of UEs per BS	3
	HARQ	Chase combining
	UE receiver	Maximum ratio combining
	Traffic model	Downlink only, full buffer
	CQI report period	5 ms
	CQI report delay	8 ms
LBT parameters	CCA slot size	9 μs
	Minimum/ maximum back-off window size	32/1024 CCA slots
	Back-off window size increment criteria of the BS	When more than 80 % of the transport blocks in a subframe fail to transmit [10]
	MCOT	7 ms
CSTA parameters	Target TFP β_{TFP}	0.13
	Minimum CST $CST_{\min}$	-91 dBm
	Maximum CST $CST_{\max}$	-53 dBm
	Learning rate α	0.8
	Exploration probability ε	0.3
	Discount factor for the EMA ω	5
	Duration between the decision epoch λ	100 ms
	Number of possible CST values $N_{\mathcal{P}}$	12
	Number of the decision epochs for training N_{tr}	30
	Number of the decision epochs $N_{\mathcal{T}}$	60

The simulation parameters used in this study are summarized in Table 1, including the specific channel model parameters, system configurations, and the LBT parameters commonly used in the proposed and conventional schemes.

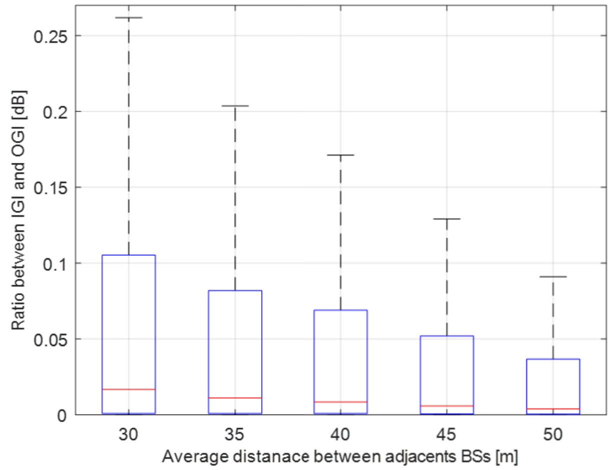

FIGURE 8. Box plot of $10\log_{10}(1 + I_{OGI}/I_{IGI})$ with varying d_{BS}.

As aforementioned, the grouping boundary must be set to d_{limit} by considering the minimum RSS, denoted by $T_{\min}$, which is subsequently determined by the transmit power. Then, let $D_{\max}$ denote the corresponding maximum CSR. We seek to set d_{limit} such that the required CSR of the header BS does not exceed $D_{\max}$. Herein, CSR is maximized when there are only two BSs in a group, including one for the header BS. Then, the distance between these two BSs is d_{limit}. This is the worst case in the sense that CSR is maximized by minimizing IGI. In this simulation, we seek to set an appropriate d_{limit} so that the CSR required in the worst case is less than $D_{\max}$. According to [22], under the assumption that the BSs are distributed by PPP, total interference can be approximated into the strongest interference. Therefore, in order for two BSs in a group to be the strongest interferers against each other, we set the CSR of the header BS to $3d_{limit}$ in the worst case, i.e., $3d_{limit} < D_{\max}$. Referring to the minimum detection strength of LTE CRS in [18], we set $T_{\min} = -92$ dBm. Furthermore, according to the transmit power and UMi NLoS path-loss model, $D_{\max}$ is approximately 375 m. Therefore, d_{limit} is set to 125 m to satisfy $3d_{limit} < D_{\max}$. Additionally, the parameters used for CST control algorithm (CSTA) are summarized in Table 1.

In the current simulation studies, to observe the performances of the conventional scheme according to frequency reuse degree, the performances of the conventional scheme are evaluated for different CST values: −52dBm, −62 dBm, and −82 dBm.

B. SIMULATION RESULTS

We first consider the scenario of a single MNO. Herein, we compare the performance when the MNO employs either the proposed scheme or the conventional scheme. Recall that a degree of CQI mismatch in the group-wise LBT is indicated by the ratio between IGI and OGI (see (7)). To ensure that the proposed scheme reduces the effect of randomly incurring OGI in the received SINR, we sample $10\log_{10}(1 + I_{OGI}/I_{IGI})$ in (7) for each UE. Fig. 8 presents a

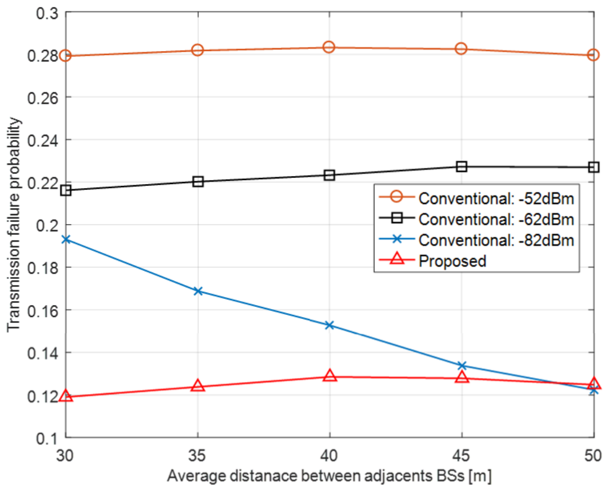

FIGURE 9. Average TFP per UE with varying d_{BS}.

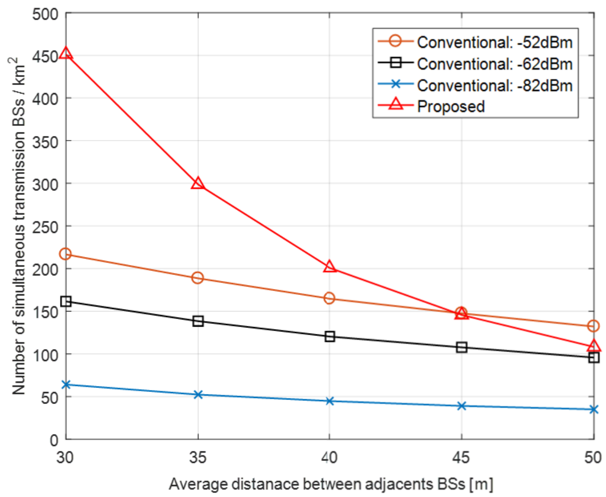

FIGURE 10. Average reuse degree with varying d_{BS}.

boxplot of the samples with varying average distance between adjacent BSs (d_{BS}) [23]. Each sample is computed by taking the time average over one subframe. On each box, the red line indicates the median, whereas the bottom and top edges of the box indicate the 25th and 75th percentiles of the sample data, respectively. Moreover, the whiskers extend to the most extreme data points not considered outliers. Herein, we consider points as outliers if they are greater than $q_3 + 1.5(q_3 - q_1)$ or less than$q_1 - 1.5(q_3 - q_1)$, where q_1 and q_3 are the 25th and 75th percentiles of the sample data, respectively [23]. We observe in Fig. 8 that most samples of $10\log_{10}(1 + I_{OGI}/I_{IGI})$ are less than 0.3 dB regardless of d_{BS}. According to the LTE standard, since the required minimum SINR value should be increased by approximately 1.5 to 3 dB to step up one MCS level, the current observation ensures that our proposed scheme can sufficiently reduce the detrimental effect of a randomly generated OGI on the received SINR.

The average TFP of the UE is shown in Fig. 9 for varying d_{BS} to demonstrate that the scheme reduces CQI mismatch while boosting the proposed spatial reuse gain. We first note that TFP for the conventional scheme with a CST of −82 dBm decreases with BS density. This is because a stringent CST induces less frequent MAC collision as the number of contention BSs in the CSR decreases. However, the conventional scheme with a CST of −52 dBm and −62 dBm show the high TFP regardless of the BS density. In this case, even if the number of contented BSs decreases, CQI mismatch occurs frequently because of hidden nodes associated with aggressive frequency reuse. This implies that CQI mismatch becomes critical in the existing DSS system, especially when subject to more aggressive frequency reuse. In contrast, the proposed scheme shows the lowest TFP (0.12 to 0.13), satisfying the target TFP (0.13) regardless of the BS density. This indicates that CQI mismatch can be controlled at the desired level even while actively reusing the channel as intended in the proposed scheme.

Recall that the areal capacity of the proposed scheme depends on the reuse degree. Therefore, before investigating its areal capacity, we compare the reuse degrees of the proposed and conventional schemes as varying d_{BS}. Fig. 10 shows the average reuse degree, which is defined as the average number of concurrent transmission BS per unit area (i.e., 1 km^2) in each subframe. It is computed by taking the time average over the simulation run time. First, we find that the conventional scheme with a CST of −52 dBm has the highest reuse degree when the ISD is more than 45 m, which is attributed to its more aggressive frequency reuse. However, it does not satisfy the target TFP as observed in Fig. 9. Investigating the best performance of the conventional scheme first, we have found that it must be set to the CST of −82 dBm, achieving the lowest TFP performance. Compared with the conventional scheme with a CST of −82 dBm, the proposed scheme shows higher performance in the reuse degree regardless of d_{BS}. In particular, its performance improves significantly with BS density, as the required CSR of the proposed scheme decreases with the distance between BSs in the group. Together with the results in Fig. 9, those in Fig. 10 ensure that the proposed scheme can increase the reuse degree while satisfying the target TFP with CSTA.

Subsequently, Fig. 11(a) shows the average areal capacity with varying d_{BS} (m). We first note that the areal capacity of the proposed scheme is highly consistent with the reuse degree of the proposed scheme in Fig. 10, as expected. Note that Fig. 11(b) presents the same result in the explicit form of areal capacity, i.e., the number of BSs/km^2. Using the slopes of the graph in Fig. 11(b), the average BS capacities are estimated as 9.68 and 2.19 Mbps/BS for the proposed and conventional schemes with a CST of −82 dBm, respectively. This corresponds to an almost 4.42 times enhancement in the areal capacity gain of the proposed scheme over the conventional scheme.

Finally, we intend to determine if two different systems that employ the proposed scheme and the conventional scheme

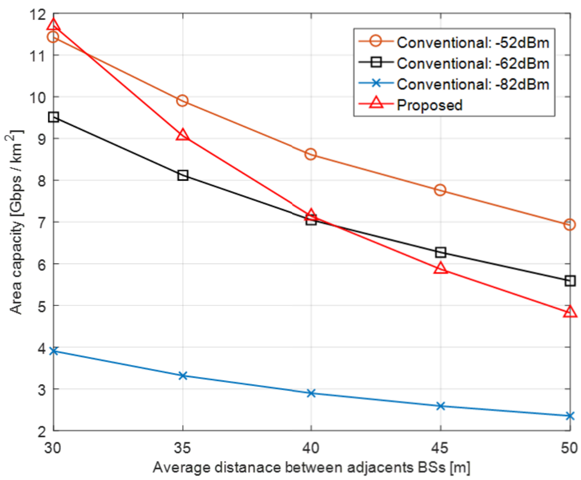

(a) Areal capacity with varying d_{BS}

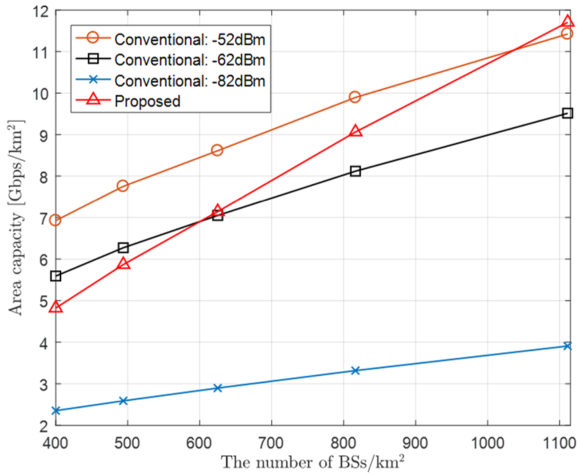

(b) Areal capacity with varying BS density

FIGURE 11. Average areal capacity with varying: (a) d_{BS}, (b) BS density.

are allowed to coexist using the same channel. To evaluate this scenario, we borrow a notion of *fair coexistence* in the 3GPP-LAA standard [19]. To define fair coexistence, we consider the following two different scenarios, particularly with two operators designated as MNO A and MNO B:

- **Scenario 1**: MNO A with the conventional scheme vs. MNO B with the conventional scheme.
- **Scenario 2**: MNO A with the conventional scheme vs. MNO B with the proposed scheme.

Herein, the notion of fair-coexistence dictates that the performance of MNO A with the conventional scheme under Scenario 2 should perform at least as well as MNO A with the conventional scheme under Scenario 1. For the coexistence scenario, 20 BSs of MNO A and 80 BSs of MNO B are uniformly distributed in the square space with an area of 300 m x 300 m. Herein, the CST of the conventional scheme is set to −82 dBm. Meanwhile, we design CSTA considering the TFP of the BSs that belong to the same MNO. Therefore, if header BS in MNO B applies CST derived from CSTA regardless of MNO, it may degrade the performance of the

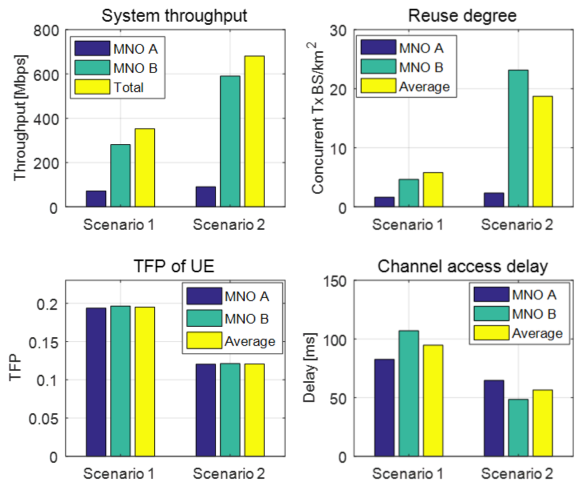

FIGURE 12. Performance comparison under coexistence scenarios.

MNO adopting the conventional scheme. Therefore, in Scenario 2, the header BSs perform CS by setting the CST to −82 dBm for the interference sources of MNO A. In addition, for the interference sources of the same operator (MNO B), the header BSs use the CST derived from the CSTA. This method is similar to the energy detection threshold adaptation (EDTA) specified in the LAA standard. To protect the Wi-Fi system, it sets energy detection threshold to the maximum value provided the Wi-Fi system does not occupy the channel [10]. Meanwhile, we set the MCOT of the MNO A to 7 ms. Here, in Scenario 1, since both MNOs adopt the conventional scheme, the MNO B set the MCOT to 7 ms. Also, for fair performance comparison of MNO B according to the above scenarios, we set the MCOT of proposed scheme to 14 ms so that the system throughput of MNO A in Scenario 1 and that of MNO A in Scenario 2 show similar value.

VII. CONCLUSION

Over the past decades, a common-sense approach to overcome the hidden node problem in the existing downlink DSS system has been confined to avoiding interference or relying on link adaption based on the previous transmission history, and various techniques have been developed based on these approaches. In this paper, we argue that its fundamental limitation is the result of the uncoordinated channel access mechanism, which ultimately suffers from the unpredictable and random nature of co-channel interference. To overcome this limitation, we buck the trend of the existing DSS system by inducing a strong fixed interference pattern within a group of BSs. Specifically, by leveraging the feature of the coordinated DSS system, we consider a group-wise LBT protocol that can increase areal capacity in the DSS environment. It is unified into a complete coordination framework with elementary algorithms for BS grouping and CST adjustment. Our system-level simulation results demonstrate that the proposed framework can improve its areal capacity over the conventional DSS approach by 4.42 times, indicating a substantial saving in mobile infrastructure cost.

Even though we only consider the downlink DSS system, the current design principle can still be extended to an uplink DSS system. However, due to the structural differences between the downlink and uplink in the cellular system, the implementation framework in this paper may not be extended in a straightforward manner. Thus, we leave this issue as our future work. We expect that the proposed framework will be a new milestone for the system design in various future DSS scenarios.

REFERENCES

[1] A. M. Voicu, L. Simic, and M. Petrova, "Survey of spectrum sharing for inter-technology coexistence," *IEEE Commun. Surveys Tuts.*, vol. 21, no. 2, pp. 1112–1144, 2nd Quart., 2019.

[2] M. D. Mueck, V. Frascolla, and B. Badic, "Licensed shared access—State-of-the-art and current challenges," in *Proc. 1st Int. Workshop Cognit. Cellular Syst. (CCS)*, Berlin, Germany, Sep. 2014, pp. 1–5.

[3] S. Kim, S. Yoo, J. Yi, Y. Son, and S. Choi, "FACT: Fine-grained adaptation of carrier sense threshold in IEEE 802.11 WLANs," *IEEE Trans. Veh. Technol.*, vol. 66, no. 2, pp. 1886–1891, Feb. 2017.

[4] L. Fu, S. C. Liew, and J. Huang, "Effective carrier sensing in CSMA networks under cumulative interference," *IEEE Trans. Mobile Comput.*, vol. 12, no. 4, pp. 748–760, Apr. 2013.

[5] T.-S. Kim, H. Lim, and J. C. Hou, "Understanding and improving the spatial reuse in multihop wireless networks," *IEEE Trans. Mobile Comput.*, vol. 7, no. 10, pp. 1200–1212, Oct. 2008.

[6] Q. Xia, M. Hamdi, and K. Ben Letaief, "Open-loop link adaptation for next-generation IEEE 802.11n wireless networks," *IEEE Trans. Veh. Technol.*, vol. 58, no. 7, pp. 3713–3725, Sep. 2009.

[7] K. Yoon, W. Sun, and S. Choi, "COALA: Collision-aware link adaptation for LTE in unlicensed band," in *Proc. 15th Annu. IEEE Int. Conf. Sens., Commun., Netw. (SECON)*, Hong Kong, Jun. 2018, pp. 1–9.

[8] M. Labib, V. Marojevic, J. H. Reed, and A. I. Zaghloul, "Extending LTE into the unlicensed spectrum: Technical analysis of the proposed variants," *IEEE Commun. Standards Mag.*, vol. 1, no. 4, pp. 31–39, Dec. 2017.

[9] C. S. Yang, C. K. Kim, J. M. Moon, S. H. Park, and C. G. Kang, "Channel access scheme with alignment reference interval adaptation (ARIA) for frequency reuse in unlicensed band," *IEEE Access*, vol. 6, pp. 26438–26451, May 2018.

[10] *Physical Layer Procedures*, document TS 36.213 v14.4.0, 3GPP, Sep. 2017.

[11] *UE Radio Transmission and Reception*, document TS 36.213 v15.4.0, 3GPP, Sep. 2018.

[12] J. Zander, "Beyond the ultra-dense barrier: Paradigm shifts on the road beyond 1000x wireless capacity," *IEEE Wireless Commun.*, vol. 24, no. 3, pp. 96–102, Jun. 2017.

[13] *Potential Designs to Support Spatial Reuse for NR-Unlicensed*, document R1-1806548, 3GPP, Intel Corporation, Santa Clara, CA, USA, May 2018.

[14] J. G. Andrews, F. Baccelli, and R. K. Ganti, "A tractable approach to coverage and rate in cellular networks," *IEEE Trans. Commun.*, vol. 59, no. 11, pp. 3122–3134, Nov. 2011.

[15] A. P. Reynolds, G. Richards, B. de la Iglesia, and V. J. Rayward-Smith, "Clustering rules: A comparison of partitioning and hierarchical clustering algorithms," *J. Math. Model. Algorithms*, vol. 5, no. 4, pp. 475–504, Mar. 2006.

[16] H.-S. Park and C.-H. Jun, "A simple and fast algorithm for K-medoids clustering," *Expert Syst. Appl.*, vol. 36, no. 2, pp. 3336–3341, Mar. 2009.

[17] W. Wang, A. Kwasinski, D. Niyato, and Z. Han, "A survey on applications of model-free strategy learning in cognitive wireless networks," *IEEE Commun. Surveys Tuts.*, vol. 18, no. 3, pp. 1717–1757, 3rd Quart., 2016.

[18] *Requirements for Support of Radio Resource Management*, document TS 36.133 v16.2.0, 3GPP, Jun. 2019.

[19] *Study on Licensed-Assisted Access to Unlicensed Spectrum*, document TR 36.889 v1.0.1, 3GPP, Jun. 2015.

[20] C. K. Kim, C. S. Yang, and C. G. Kang, "Adaptive Listen-Before-Talk (LBT) scheme for LTE and Wi-Fi systems coexisting in unlicensed band," in *Proc. 13th IEEE Annu. Consum. Commun. Netw. Conf. (CCNC)*, Las Vegas, NV, USA, Jan. 2016, pp. 589–594.

[21] *Further Analysis on LBE Options for Reuse-1 LAA*, document R1-153415, 3GPP, Samsung, Seoul, South Korea, May 2015.

[22] Y. Li, F. Baccelli, J. G. Andrews, T. D. Novlan, and J. C. Zhang, "Modeling and analyzing the coexistence of Wi-Fi and LTE in unlicensed spectrum," *IEEE Trans. Wireless Commun.*, vol. 15, no. 9, pp. 6310–6326, Sep. 2016.

[23] MathWorks. *Boxplot*. Accessed: Feb. 5, 2020. [Online]. Available: https://kr.mathworks.com/help/stats/boxplot.html?lang=en

CHAN S. YANG received the B.S. and M.S. degrees in electrical engineering from Korea University, Seoul, South Korea, in 2012 and 2014, respectively, where he is currently pursuing the Ph.D. degree. His research interests include next-generation mobile radio communication systems, dynamic spectrum sharing, frequency reuse-1 in unlicensed bands, machine learning, and wireless resource management.

CHUNG G. KANG (Senior Member, IEEE) received the B.S. degree in electrical engineering from the University of California at San Diego, San Diego, CA, USA, in 1987, and the M.S. and Ph.D. degrees in electrical and computer engineering from the University of California at Irvine, Irvine, CA, USA, in 1989 and 1993, respectively. Since March 1994, he has been with the Department of Radio Communication and Engineering and the Department of Electrical Engineering, Korea University, Seoul, South Korea, where he is currently a Full Professor. He has published over 200 refereed publications in international journals and conference proceedings in the fields of mobile communication and wireless networks. He has coauthored a reference textbook on the MIMO-OFDM wireless systems, entitled *MIMO-OFDM Wireless Communications with MATLAB* (Wiley, 2010). He holds over 90 patents. His research interests include next-generation mobile radio communication systems and broadband wireless networks with an emphasis on cross-layer design and optimization, massive MIMO, grant-free non-orthogonal multiple access, dynamic spectrum access, mobile caching networks, and AI-based communication system design. He is a Senior Member of the IEEE COMSOC, the IEEE IT, and the IEEE VT, a Life-Time Member of KICS, and a Regular Member of the National Academy of Engineering of Korea. He was a recipient of the Dr. Irwin Jacobs Award sponsored by Qualcomm Inc. for his contribution to research on mobile communication technologies. He served as the Chair for the 2.3GHz IMT-WiBro Project Group (PG702) in Telecommunications Technology Association (TTA), which is a standard development organization (SDO) in South Korea, the KICS Mobile Communication Technical Activity Group, and the Wireless Technology Committee in 5G Forum of Korea. He has also served as the President of KICS.